





## Quantifying exchange effects in incommensurate solid $^4\text{He}$

R. Almeida <sup>1</sup>, B. G. A. Brito <sup>2</sup>, G.-Q. Hai <sup>3</sup> and L. Cândido <sup>1,\*</sup>

<sup>1</sup>*Instituto de Física, Universidade Federal de Goiás, 74001-970, Goiânia, Goiás, Brazil*

<sup>2</sup>*Departamento de Física, Instituto de Ciências Exatas e Naturais e Educação (ICENE), Universidade Federal do Triângulo Mineiro - UFTM, 38064-200, Uberaba, Minas Gerais, Brazil*

<sup>3</sup>*Instituto de Física de São Carlos, Universidade de São Paulo, 13560-970, São Carlos, São Paulo, Brazil*



(Received 25 March 2024; revised 28 May 2024; accepted 6 June 2024; published 21 June 2024)

In this paper, we use path-integral Monte Carlo (PIMC) simulations to study how the permutation effect, a specific quantum exchange phenomenon, affects the stability of incommensurate solid  $^4\text{He}$  with vacancy defects. By comparing simulations within Bose and Boltzmann statistics, we isolate the effects of quantum exchange. We examine the solids with densities from  $0.028$  to  $0.035 \text{ \AA}^{-3}$  and vacancy concentrations from  $0.55$  to  $5.55\%$  in the temperature range  $0.2$ – $2.0 \text{ K}$ . The calculations show that permutations reduce the vacancy formation energy by up to  $19\%$ , especially at lower densities. Vacancies in the studied concentration range can lead to lattice distortions with a reduction in the local density of  $1\%$  to  $5\%$  and a compensatory increase in the neighboring regions. The Bose statistics influence the local atomic arrangement, which is reflected in the pair-correlation function, with the peaks and valleys changing by about  $2\%$  at larger distances. Permutation effects on the vacancy formation energy show a dependence on density and temperature with “steplike behavior”. Our results demonstrate that quantum statistics play a significant role in shaping the structure and stability of solid  $^4\text{He}$ -containing vacancies.

DOI: [10.1103/PhysRevB.109.224513](https://doi.org/10.1103/PhysRevB.109.224513)

### I. INTRODUCTION

$^4\text{He}$ , known for its quantum phenomena, exhibits several anomalous behaviors that distinguish it from conventional materials. In particular, it exhibits phenomena such as superfluidity and Bose-Einstein condensation (BEC) in the liquid phase, the ability to remain liquid at absolute zero, and significant zero-point motion in the solid phase. The conundrum becomes even greater when we face the challenge of solidifying helium at absolute zero, which is only possible under external pressure, typically around  $25$  atmospheres. This necessity arises from the unique properties of helium, its low atomic mass, its weak interatomic potential, and its pronounced zero-point motion. The resulting phase diagram is strongly influenced by quantum effects, making mean-field theories and perturbation approaches inadequate. Solid helium thus becomes a ubiquitous system for studying the properties of quantum solids.

Despite the elusive evidence of solid helium with superfluid properties, experimental efforts have revealed remarkable properties such as giant plasticity and mass flow [1–4]. In recent years, attention has shifted to metastable solid  $^4\text{He}$ , a phenomenon that has only been observed relatively recently [5–7]. Theoretical studies aimed at understanding the stability limit have been concerned with determining the spinodal pressure of solid hcp  $^4\text{He}$ , which often deviates significantly from experimental values due to neglected crystalline defects [8,9]. Crucially, the destabilization pressure of hcp  $^4\text{He}$  appears to be related to a heterogeneous nucleation process triggered by defects. Experimental evidence suggests that the insta-

bility arises from the repeated application of stresses to the solid, possibly leading to fatigue and defect propagation. It is hypothesized that both vacancies and dislocations contribute to fatigue in metastable states of  $^4\text{He}$  [5,7].

Solving this complex stability puzzle requires sophisticated computational approaches. However, earlier estimates of the critical density using the worm algorithm path-integral Monte Carlo (WAPIMC) method did not agree with the experimental data [10]. In particular, the calculated critical pressure for destabilization significantly underestimates the experimentally observed value of  $21 \text{ atm}$  [6]. A key factor influencing the stability of metastable  $^4\text{He}$  appears to be the presence of defects, in particular vacancies in the crystal lattice. These vacancies disrupt the ordered lattice structure and influence the interaction of the He atoms with each other. In addition, the significant zero-point motion of the  $^4\text{He}$  atoms leads to delocalization effects in which the atoms fluctuate around their lattice positions. This interplay between vacancies, atomic interactions, and quantum mechanical delocalization creates a captivating interplay that determines the stability and unique properties of the material.

In this paper, the intricate interplay between quantum effects and atomic interactions in metastable solid  $^4\text{He}$  with vacancies is investigated using path-integral Monte Carlo (PIMC) simulations. This approach allows us to accurately quantify the effects of quantum exchange (permutation) by comparing simulations performed using Bose and Boltzmann statistics. We effectively isolate the influence of bosonic statistics on two key aspects: (i) the energy of vacancy formation, which plays a crucial role in stabilizing vacancies, and (ii) the crystal lattice distortions caused by the vacancies, which provide valuable insights into the interactions between defect and structure. Our goal in this study is to improve the

\*Contact author: [ladir@ufg.br](mailto:ladir@ufg.br)

comprehensive understanding of the role of quantum effects in shaping the behavior and structure of solid  $^4\text{He}$  for densities in the range  $0.028\text{--}0.035 \text{ \AA}^{-3}$ . We pay particular attention to the importance of vacancies and their complex interaction with bosonic statistics.

## II. COMPUTATIONAL APPROACHES AND DETAILS

We use the PIMC method [11,12] in our study. In this method the quantum density matrix

$$\rho(R_0, R_M; \beta) = \int d\mathbf{R}_1 \dots d\mathbf{R}_{M-1} \exp \left[ - \sum_{m=1}^M S^m \right] \quad (1)$$

is evaluated by sampling paths  $\{\mathbf{R}_0, \mathbf{R}_1, \dots, \mathbf{R}_{M-1}, \mathbf{R}_M\}$ , where  $\mathbf{R}_k$  is the set of beads  $\{\mathbf{r}_{1,k}, \dots, \mathbf{r}_{n,k}\}$ , and  $\mathbf{r}_{i,k}$  is a bead representing the position of the  $i^{\text{th}}$  particle in the  $k^{\text{th}}$  time slice. The time step is defined as  $\tau = \beta/M$  with  $\beta = 1/k_B T$  ( $k_B$  is the Boltzmann constant and  $T$  is the absolute temperature). The action  $S^m \equiv S(\mathbf{R}_{m-1}, \mathbf{R}_m; \tau) \equiv -\ln[\rho(R_{m-1}, \mathbf{R}_m; \tau)]$  is evaluated using the exact pair action of two bodies within the matrix squaring method [12–14]. The bosonic nature of the system is described by a density matrix that takes into account the summation of all permutations ( $P$ ) of the particle labels

$$\rho_B(R_0, R_M; \beta) = (N!)^{-1} \sum_P \rho(R_0, PR_M; \beta). \quad (2)$$

The evaluation of both the integral over the paths [Eq. (1)] and the sum over the permutations [Eq. (2)] is performed by a generalized Metropolis algorithm using the bisection sampling technique [12,15].

The Hamiltonian used to describe a system of  $N$  atoms of  $^4\text{He}$  is given by

$$H = -\lambda \sum_{i=1}^{N_a} \nabla_i^2 + \sum_{i<j} V(\mathbf{r}_{ij}), \quad (3)$$

where  $\lambda = \hbar^2/2m = 6.059615 \text{ \AA}^2 \text{ K}$ ,  $m$  is the  $^4\text{He}$  mass, and  $V$  is the interatomic helium potential proposed by Aziz and coworkers [16].

Our PIMC simulations using the UPI code [12] employ a standard permutation scheme, which is well suited for solid  $^4\text{He}$ , rather than the worm algorithm [17] for permutation updates. While the worm algorithm efficiently handles winding number exchanges in systems with many particles, it is optimized for quantum fluids, not solids like  $^4\text{He}$ , which lack the superfluid characteristics necessary for such exchanges. Additionally, we have enhanced efficiency by implementing a selective sampling strategy. This approach prioritizes permutations that are most likely to significantly impact the partition function, thereby reducing computational overhead and increasing the overall effectiveness of our simulations. Also, the simulations are performed by using a specifically designed three-dimensional box with periodic boundary conditions to accommodate a hexagonal close-packed (hcp) lattice of 180 sites. The hcp  $^4\text{He}$  crystals under investigation are of densities in the range  $0.028\text{--}0.035 \text{ \AA}^{-3}$  and temperatures from 0.2 to 2.0 K. The simulation box contains 0 to 10 vacancies, initially distributed randomly within it. From a large number of samples obtained through this approach, we strategically select specific vacancy configurations to gain insights into vacancy

effects. This strategic selection enables a systematic investigation of general trends that are crucial to understanding the interplay between vacancies, quantum effects, and crystal density in Bose systems.

The introduction of vacancies into the  $^4\text{He}$  crystal distorts the lattice structure. The extent of this distortion provides information about the spatial delocalization of the quantum vacancy within the crystal. To circumvent the complications arising from the large lattice relaxation and zero-point motion due to vacancies, we opted for independent PIMC runs with varying particle number instead of using the more efficient insertion/removal methods [18]. Although this direct approach is computationally expensive due to the high accuracy required for energy difference calculations in large systems, it provides better control over systematic errors.

Checks with a larger system (384 atoms) confirmed results convergence and no significant deviations from the smaller system (180 atoms), ensuring reliability. Most of the calculations achieved converged results within the error bars employing discretized imaginary time path integrals with a time step of  $\tau = 0.0125 \text{ K}^{-1}$ , corresponding to 160 imaginary time slices at a temperature of 0.5 K. This time step size proved sufficient compared to a smaller value ( $\tau = 0.00625 \text{ K}^{-1}$ ), ensuring computational efficiency without compromising accuracy. In a typical simulation, at least  $4 \times 10^6$  PIMC time steps were performed.

## III. RESULTS AND DISCUSSIONS

Before examining the permutation effect on vacancy behavior, we first validate the accuracy of our PIMC results. We compare our calculations for the energy cost of creating a single vacancy in a  $^4\text{He}$  crystal at densities between  $0.028 - 0.035 \text{ \AA}^{-3}$  to available theoretical and experimental results. This approach helps to ensure the reliability of our calculations. In some crystalline materials, including potentially solid  $^4\text{He}$ , introduction of a vacancy can lead to a more stable state (lower overall free-energy state), especially at low temperatures and low-vacancy densities. This phenomenon results from the complex interplay between lattice structure, defect formation, and entropic contributions. To quantify this energy change, we use the vacancy formation energy  $E_v$ , which represents the energetic difference between a perfect crystal and a crystal with a single vacancy. We calculate  $E_v$  using the following definition:

$$E_v = E(N-1) - \frac{N-1}{N} E(N), \quad (4)$$

where  $E(N)$  and  $E(N-1)$  represent the total energies of the perfect crystal and the crystal with a single vacancy, respectively, at the same density  $\rho$ . Both simulation boxes are set to keep the same density, so the estimated  $E_v$  represents the vacancy formation energy at constant density.

In Fig. 1 we plot the vacancy formation energy  $E_v$  as a function of density  $\rho$  at  $T = 0.5 \text{ K}$ . For each calculation, we consider about 10 samples of the defective system with a single vacancy in the hcp lattice. The obtained vacancy formation energy shows an overall linear dependence on the density. Notably, a small jump in energy occurs near  $\rho = 0.032 \text{ \AA}^{-3}$ , potentially indicating a lattice restructuring.

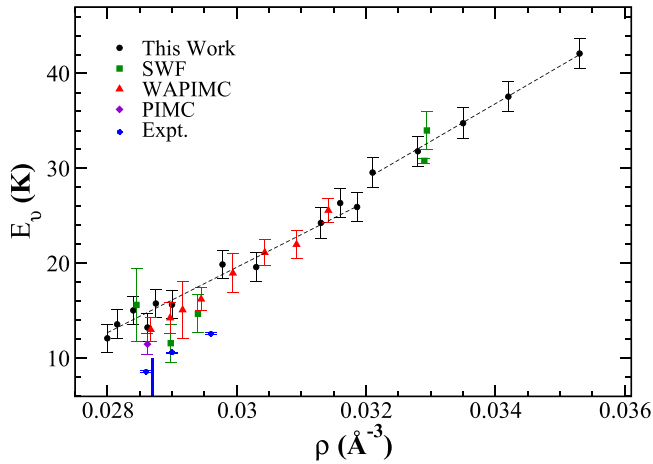


FIG. 1. Vacancy formation energy as a function of the crystal density. The results from our PIMC calculations are given by the black dots. Also shown previous theoretical calculations (the green squares from the SWF calculation [19–21], purple diamonds from PIMC [22], and red triangles from WAPIMC [23]), experimental results (the blue dots) and experimental melting density (vertical solid line) from Ref. [24]. The dashed lines are a linear fit of the data.

Interestingly, data below this density exhibit increased scatter, possibly due to the complicated interplay between metastability and increasing permutation. Our results agree well with previously published calculations using various methods as shown in the figure, including those of variational shadow wave function (SWF) [19–21], WAPIMC [23], and PIMC [22]. Although the trend is consistent with available experimental data, our calculation yields a larger vacancy formation energy.

### A. Permutation effect

At finite temperatures, the statistics become relevant and significantly influence the internal energy of the system. In PIMC simulations of solid  $^4\text{He}$ , we implement Bose statistics through cyclic permutations of the particle paths, reflecting the indistinguishability of the atoms. The introduction of a vacancy in the lattice significantly increases the probability of such permutations around the defect [22]. This increased occurrence offers important insight into the influence of bosonic exchange on the behavior of defects, particularly on the interaction and motion of vacancies in the crystal.

In the following discussion of the obtained thermodynamic and structural results, we attempt to quantify this permutation effect, which is crucial for a comprehensive understanding of the properties of the system. To this end, we perform separate simulations using both Boltzmann and Bose statistics, explicitly considering the permutations in the latter. By subtracting the result obtained within the Boltzmann statistics as a reference, we can isolate the additional contribution of the Bose statistics, which includes the permutation effects and any inherent differences in the statistical treatment.

This approach allows us to distinguish the specific role of permutations from other bosonic effects on vacancy dynamics and provides valuable insights into the thermodynamic and structural properties of the solid  $^4\text{He}$  with vacancy defect.

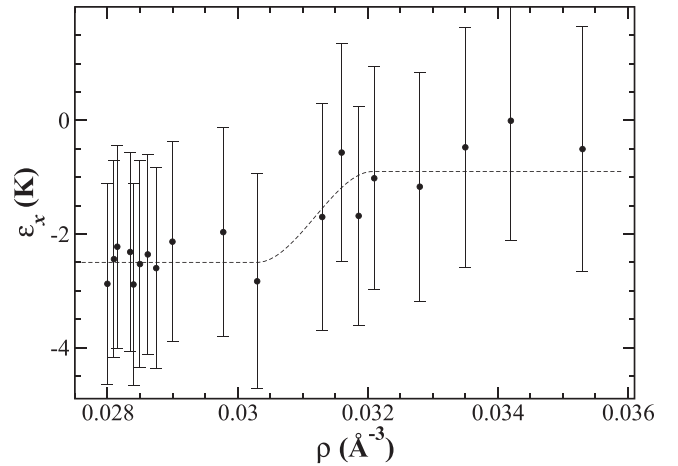


FIG. 2. Permutation contribution to the vacancy formation energy as a function of crystal density at  $T = 0.5$  K. The dashed line is only a guide for the eyes.

### 1. Thermodynamic analysis

To quantitatively investigate the influence of permutations on vacancy formation, we examine the energy difference

$$\varepsilon_x = E_v^{\text{BS}} - E_v^{\text{BZ}}, \quad (5)$$

where  $E_v^{\text{BS}}$  and  $E_v^{\text{BZ}}$  are the vacancy formation energies calculated within the Bose and Boltzmann statistics, respectively.

Figure 2 shows that  $\varepsilon_x$  has consistently negative values, indicating that permutations effectively lower the energy of the vacancy formation in this system. Two different regimes arise: at higher crystal density ( $\gtrsim 0.032 \text{ \AA}^{-3}$ ) permutations contribute  $-0.9 \pm 2.0$  K to the formation energy, reflecting a moderate stabilization effect. On the other hand, permutations at lower density ( $\lesssim 0.032 \text{ \AA}^{-3}$ ) have a stronger impact and reduce the formation energy by  $-2.5 \pm 1.8$  K, indicating a more significant role in stabilizing the vacancy (a rough estimate of the permutation effect suggests that it is responsible for about 19% of the total value of  $E_v$  in this range of crystal density). Although the sizable error bars (about 2.0 K) overlap with the permutation contributions in both density ranges, highlighting the difficulties in determining precise quantitative nuances, the general trend and quantified values of the permutation effect provide insight into its density-dependent influence on the vacancy formation. Clark and Ceperley [22] found in a single calculation for  $\rho = 0.02862 \text{ \AA}^{-3}$  that the delocalization caused by turning on the Bose statistics in a system with vacancies lowers the total energy by about  $2 \sim 3$  K, which is consistent with our results. These results emphasize the density-dependent nature of the permutation effects on vacancy formation in this bosonic quantum crystal.

The temperature effect on the permutation contribution to the vacancy formation energy ( $\varepsilon_x$ ) is analyzed at a fixed density of  $0.02862 \text{ \AA}^{-3}$  with a single vacancy  $n_v = 1$  (corresponding to a vacancy concentration of 0.55%). Figure 3 shows a clear trend that for  $T \lesssim 1.0$  K the exchange permutations lower significantly the vacancy formation energy by about 2.5 K. This trend is also supported by the lower standard errors in the lower-temperature range 1.8 K in comparison to 2.2 K error at higher temperatures, indicating a potentially

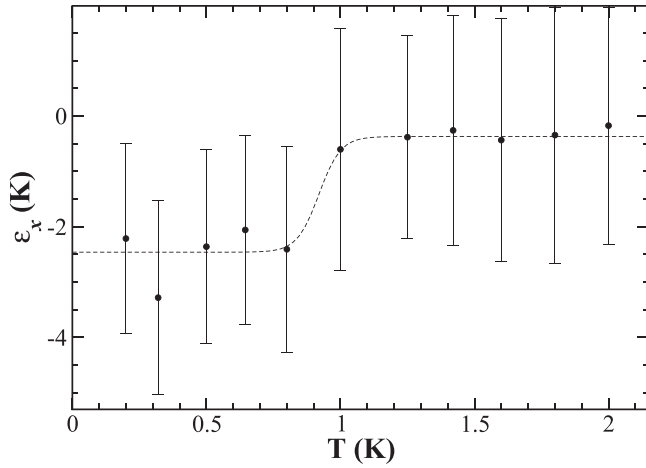


FIG. 3. Permutation contribution to the vacancy formation energy as a function of temperature at  $\rho = 0.02862 \text{ \AA}^{-3}$ . The dashed line is only a guide for the eyes.

higher confidence in the PIMC calculations. Interestingly, the average permutation value drops sharply from  $-0.4 \text{ K}$  to  $-2.5 \text{ K}$  at the boundary of  $0.8 \sim 1.0 \text{ K}$ . This rapid change could be related to the behavior of vacancies and the presence of a finite condensation fraction, similar to that observed for FCC and BCC lattices at similar densities [25]. Notice that in previous studies [25,26] the condensation fraction of  $\sim 10^{-3}$  was estimated at  $0.5 \text{ K}$  based on a one-body density matrix analysis. Our rough estimates, based on the hypothesis of Hyland *et al.* [27] assuming that above  $1.0 \text{ K}$  the condensed fraction vanishes, suggest a condensation fraction of  $\sim 4 \times 10^{-4}$  at  $0.5 \text{ K}$ , approximately one order of magnitude lower than the reported value for FCC and BCC lattices. Although further investigation is required for more accurate estimates, this alignment indicates agreement with the presence of a finite condensate at lower temperatures.

Following the analysis of the permutation contribution to vacancy formation energy (Figs. 2 and 3), which showed a significant decrease at lower temperatures and densities, we examined permutation cycles in more detail. Permutation cycles quantify the exchange of particles in a system, which is crucial for understanding the properties of quantum systems like solid  $^4\text{He}$  with vacancies.

To quantify the excess number of permutation cycles induced by vacancies, we calculated the average weighted difference in  $n$ -cycles between the vacancy system and the perfect system, given as

$$\Delta d_n = (d'_n - d_n)w_n \quad (6)$$

with  $d_n = Nc_n/n$  and  $d'_n = (N-p)c'_n/n$ , the average number of  $n$ -cycles in the perfect and the vacancy systems, respectively, where  $c_n$  is the cycle distribution for the perfect system with  $N$  atoms and  $c'_n$  for the system with  $p$  vacancies and  $N-p$  atoms, and  $w_n$  is the weighting factor for  $n$ -cycles. This analysis was performed for various cycle sizes (including 2-cycles, 3-cycles, 4-cycles, and other  $n$ -cycles) across a temperature range from  $0.2$  to  $1.42 \text{ K}$ . We focused on 5-cycle, the most prevalent around the critical temperature range  $0.8\text{--}1.0 \text{ K}$ . For the average, we considered ten samples of the

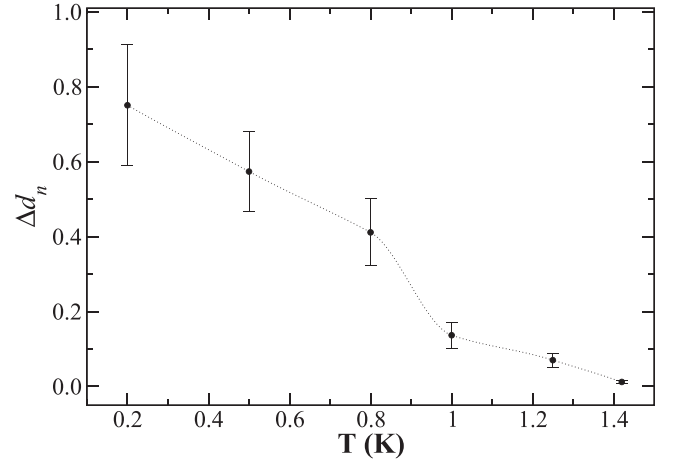


FIG. 4. Average excess number of 5-cycles induced by a single vacancy as a function of temperature at  $\rho = 0.02862 \text{ \AA}^{-3}$ . The dashed line is a guide for the eyes.

defective system, and for the weight factor, we used the cycle size  $n$  itself. This calculation involves normalization within the average number of cycles for each system, ensuring a fair comparison of cycles across different sizes and allowing us to compare different samples effectively.

Figure 4 shows the average excess number of cycles (of size 5) induced by a single vacancy as a function of temperature at  $\rho = 0.02862 \text{ \AA}^{-3}$ . At lower temperatures ( $0.2 - 0.8 \text{ K}$ ), the average excess cycles are relatively high, indicating pronounced quantum exchange activity. This aligns with the observation that exchange permutations significantly lower the vacancy formation energy by about  $2.5 \text{ K}$  for temperatures below  $1.0 \text{ K}$ , as discussed earlier. At  $0.2 \text{ K}$ , the excess number of cycles is  $0.7505$ , and it decreases to  $0.4115$  at  $0.8 \text{ K}$ , indicating a reduction in quantum exchange activity as temperature increases. At  $1.0 \text{ K}$ , the average excess cycles drop further to  $0.1366$ , about one-third of the value at  $0.8 \text{ K}$ . This significant decrease corresponds to the observed rapid drop in the permutation contribution to the vacancy formation energy, suggesting a critical transition point where quantum mechanical behavior significantly shifts. As the temperature increases further ( $1.25\text{--}1.42 \text{ K}$ ), the average excess cycles continue to decrease, reaching  $0.0118$  at  $1.42 \text{ K}$ . This trend indicates a diminishing influence of quantum exchange effects as thermal energy becomes more dominant, leading to classical vacancy behavior. The steady decline in excess cycles and low standard errors at higher temperatures confirm the reduced role of exchange permutations in this regime.

We now investigate how the number of vacancies influences the permutation effect on the vacancy formation energy in hcp  $^4\text{He}$  crystal. As shown in Fig. 5, a linear trend emerges in which the vacancy formation energy becomes more negative (stabilizing) as the number of vacancies increases in a hcp  $^4\text{He}$  crystal of density of  $\rho = 0.02862 \text{ \AA}^{-3}$  at temperature  $T = 0.5 \text{ K}$ . The slope of the fitted line is approximately  $-0.82 \text{ K/vacancy}$ . This means that for each additional vacancy the permutation energy becomes, on average, about  $0.82 \text{ K}$  more negative. The increased disorder caused by vacancies allows for more favorable permutations of the



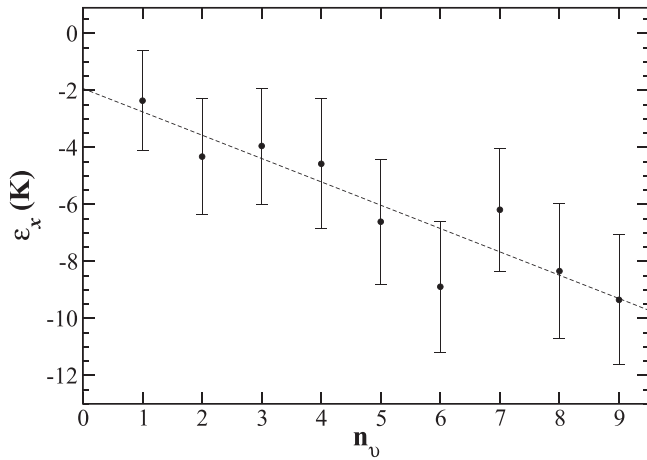


FIG. 5. Permutation contribution to the vacancy formation energy as a function of vacancy number at  $\rho = 0.02862 \text{ \AA}^{-3}$  and  $T = 0.5 \text{ K}$ . The dashed line is a linear fit of the data.

remaining atoms and further stabilizes the system. Furthermore, vacancies allow neighboring atoms to relax their positions, potentially leading to energetically preferred configurations and a stronger stabilizing effect. While the data point for the number of vacancies  $n_v = 6$  is slightly below and  $n_v = 7$  slightly above the fitted line, the deviations are likely within the margin of error. Interestingly, previous study by Clark and Ceperley [22] indicates a possible destabilization of the crystal lattice around this vacancy concentration. This finding aligns with the observed scatter in our data points for vacancies 6 and 7. However, the trend breaks down completely for ten vacancies (not shown in the graph). The data point for this higher vacancy concentration falls outside the linear regime, suggesting a strong destabilization of the lattice structure. This significant deviation warrants further investigation to understand the mechanism behind this behavior at higher vacancy concentrations. Overall, the data support the conclusion that a higher vacancy concentration results in a more negative permutation energy, contributing significantly to a lower energy cost for vacancy formation in the crystal.

## 2. Structural analysis

This section aims to quantify the influence of bosonic statistics on the atomic arrangement in the incommensurate  $^4\text{He}$  crystal. Introducing just a single vacancy into the perfect hcp lattice of the  $^4\text{He}$  crystal can lead to lattice distortion. In the context of a quantum crystal, where high zero-point motion is crucial, the vacancy region resembles a missing atomic density. This missing density is distributed over the crystal and transforms the vacancy into a delocalized unit within the  $^4\text{He}$  crystal. In its quantum nature, the delocalized vacancy is not confined to a single lattice site but exists as a wave-like function distributed over multiple sites. This property significantly reduces the vacancy dependence on a specific position within the lattice. Therefore, in such a regime delocalized vacancy interacts with a larger number of surrounding atoms through its distributed wavefunction. This interaction mitigates the individual effects of nearest neighbors and local irregularities throughout the lattice. However, even assuming

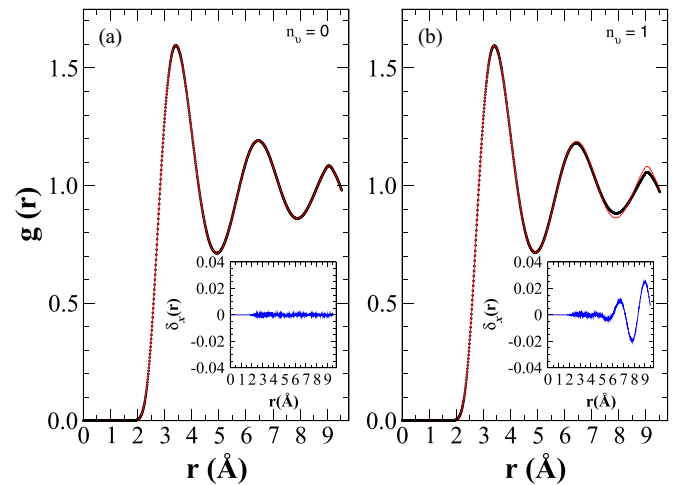


FIG. 6. Pair-correlation function for the solid at  $\rho = 0.02862 \text{ \AA}^{-3}$  and  $T = 0.5 \text{ K}$  of (a) a perfect crystal and (b) a crystal with a single vacancy. The results obtained within the Boltzmann and Bose statistics are given by the black dotted line the red solid line, respectively. The insets provide a detailed look at the differences between the pair-correlation functions, highlighting the influences of the statistics.

that the vacancy is delocalized, it is important to note that the interaction with the atoms in the neighboring layers can provoke stacking faults in the crystal on the overall arrangement of the crystal. This nuanced interplay adds more complexity for understanding the effects of vacancies in the  $^4\text{He}$  crystal.

Analyzing the pair-correlation function  $g(r)$  for perfect and vacancy-containing systems within both the Boltzmann and Bose statistics may provide valuable information on the structure of the  $^4\text{He}$  crystal. We compute the pair-density distribution for the crystals of densities from  $0.028$  to  $0.035 \text{ \AA}^{-3}$  for temperatures from  $0.2$  to  $2.0 \text{ K}$ . By comparing the results from two different statistics, we can extract the specific contributions due to Bose statistics, such as quantum exchange and long-range correlations, and quantify their influence on the crystal structure of solid  $^4\text{He}$  with vacancy defects.

Figure 6 compares the pair-correlation function  $g(r)$  for perfect and single-vacancy hcp  $^4\text{He}$  crystals within the Bose and Boltzmann statistics. It is noticeable that the statistical effects on the perfect crystal are minimal as shown in Fig. 6(a) by the almost identical  $g(r)$  curves. However, in a crystal with a single vacancy, the Bose statistics play an important role as shown in Fig. 6(b), especially for  $r > 6 \text{ \AA}$ . In comparison to the Boltzmann statistics (black-dotted line), we see higher peak and deeper valley in  $g(r)$ . The increasing deviation of  $g(r)$  at larger distances reflects the growing role of permutation effects (quantum exchange processes) in the presence of vacancies. As the distance between atoms increases, the lower momentum of the helium atoms leads to a larger de Broglie wavelength, so these exchange paths are more likely contributing to the pair correlation. While the vacancy primarily affects the local order through distortions, it could also indirectly affect the longer-range correlation. These combined effects and the absence of exchange in the Boltzmann simulation lead to the observed changes in the oscillation of the  $g(r)$

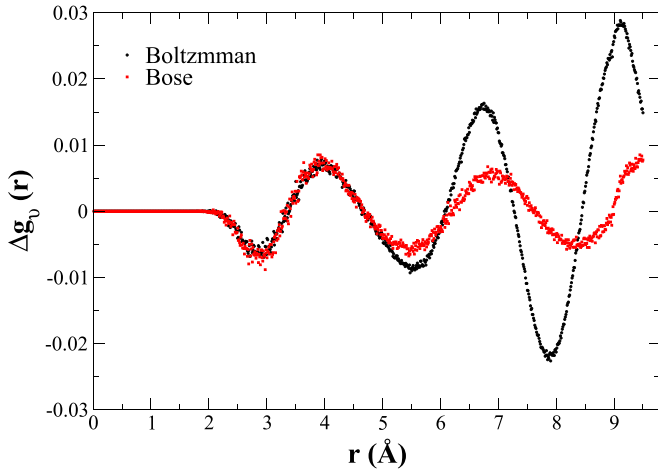


FIG. 7. Pair-correlation function difference for a system with a single vacancy at  $\rho = 0.02862 \text{ \AA}^{-3}$  and  $T = 0.5 \text{ K}$  using both Boltzmann and Bose statistics.

function. Such a difference is quantified by

$$\delta_x(r) = g^{\text{BS}}(r) - g^{\text{BZ}}(r), \quad (7)$$

where  $g^{\text{BS}}(r)$  and  $g^{\text{BZ}}(r)$  are the pair-correlation functions obtained within the Bose and Boltzmann statistics, respectively, as shown in the insets of Fig. 6. It evidences the importance of quantum exchange effects on  $g(r)$  obtained within the Bose statistics for the hcp  $^4\text{He}$  crystal with vacancy. Notably, in Fig. 6(b), the peak at  $6.5 \text{ \AA}$  is 1.1% higher and the valley in the next is 2% lower. Similarly, the third peak at  $9 \text{ \AA}$  increases by more than 2.5%, emphasizing the influence of the exchange effects at larger interatomic distances.

In order to show how vacancies affect the arrangement of the atoms in the hcp  $^4\text{He}$  crystal, we look at the difference between the pair-correlation functions of the crystal with vacancies and the perfect one without defect, given by

$$\Delta g_v(r) = g_v(r) - g_0(r) \quad (8)$$

where  $g_v(r)$  is the pair-correlation function of the  $^4\text{He}$  crystal with vacancies and  $g_0(r)$  that of a perfect crystal. As can be seen in Fig. 7, the two curves obtained within different statistics show a distinct pattern illustrating the influence of single vacancy ( $n_v = 1$ ) on the crystal structure. When a vacancy is introduced into the crystal, it creates a void where an atom used to be. Surrounding atoms may experience reduced repulsive forces due to the increased distance between them and the vacancy site. This reduction in repulsive interaction leads to a localized decrease in density around the vacancy, as atoms are not as strongly pushed away from each other as in the perfect crystal lattice. The  $\Delta g_v(r)$  function shows this as valleys, indicating areas of lower atomic density compared to the undisturbed crystal. On the other hand, in response to the vacancy, atoms in the crystal may rearrange themselves to minimize the system's overall energy. This rearrangement can lead to localized increases in density as atoms move closer to fill in the space left by the vacancy or adjust their positions to achieve a more stable configuration. These areas of increased density are seen as positive peaks in the  $\Delta g_v(r)$ , signaling attractive rearrangements of atoms around the vacancy. The

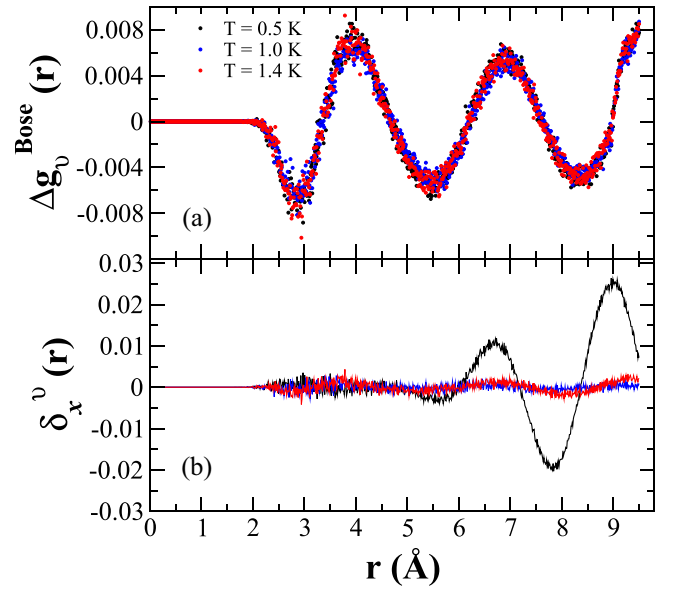


FIG. 8. (a) Pair-correlation function difference for a system with single-vacancy at three different temperatures and (b) the permutation effect on  $g(r)$ . The calculations are for a density  $\rho = 0.02862 \text{ \AA}^{-3}$ .

balance between these repulsive and attractive forces, altered by the introduction of a vacancy, dictates the new equilibrium state of the crystal structure. The function  $\Delta g_v(r)$  captures these changes, providing insight into how the vacancy influences the local atomic interactions and overall crystal stability.

At short distances up to about  $5 \text{ \AA}$ , the  $\Delta g_v(r)$  curve obtained within the Bose statistics is practically identical to that within the Boltzmann statistics. At larger distances, however, the Bose curve shows a remarkable decrease in the oscillation amplitude in comparison to the Boltzmann one. This suppression, being more significant for larger interatomic distance, indicates that in the presence of vacancy defects the quantum exchange paths in the Bose system weaken the local correlations at larger distances and reduce amplitudes of the structural rearrangements. Moreover, a shift of the Bose peaks to the right enhances the picture of delocalized atoms exploring a wider range of positions around the vacancy. This nonlocal influence emphasizes the significant reorganization of the crystal structure induced by the vacancy, the effects of which extend beyond its immediate vicinity.

In the following, we pay particular attention to the function  $\Delta g_v(r)$  obtained within the Bose statistics [denoted as  $\Delta g_v^{\text{BS}}(r)$ ]. We examine the interplay between temperature, vacancies, and permutations in the system under study. The pair-correlation function difference  $\Delta g_v^{\text{BS}}(r)$  calculated within the framework of Bose statistics is shown in Fig. 8(a). The peaks and valleys show how vacancies affect the crystal structure. Remarkably, these features remain unchanged in the temperature range  $0.5\text{--}1.4 \text{ K}$ , suggesting that vacancy-induced distortions are insensitive to these thermal fluctuations. It emphasizes the persistent role of vacancies in shaping the  $^4\text{He}$  crystal structure in this temperature range. To investigate the dynamical interplay beyond the static vacancies, we examine the permutation effect quantified by  $\delta_x(r)$

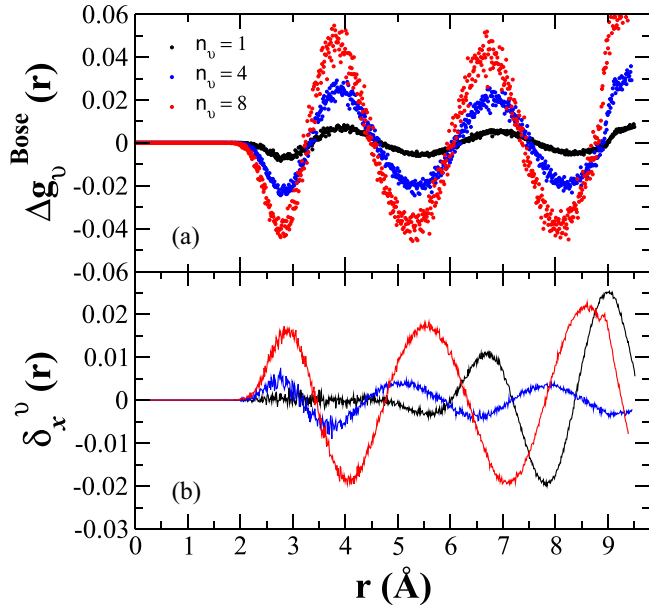


FIG. 9. (a) Pair-correlation function difference at three different vacancy numbers and (b) the permutation effect on  $g(r)$ . The calculations are for  $\rho = 0.02862 \text{ \AA}^{-3}$  and  $T = 0.5 \text{ K}$ .

[Eq. (7)] computed as the difference between the  $g(r)$  of crystals with single-vacancy. The obtained  $\delta_x(r)$  is presented in Fig. 8(b), illustrating the influence of the permutation caused by the vacancy. Interestingly, the figure shows a temperature-dependent permutation effect, which is most pronounced at larger distances and lower temperatures ( $0.5 \text{ K} \sim 0.8 \text{ K}$ ). In this range, permutations increase the  $g(r)$  peaks by up to 2%. With increasing temperature ( $\geq 1.0 \text{ K}$ ), their influence suddenly becomes negligible. The observed temperature dependence is consistent with earlier findings on the “steplike behavior” of the permutation contribution to vacancy formation energy. This means that the importance of the permutation effect decreases when the  $^4\text{He}$  crystal experiences a higher thermal energy. This underlines the complicated interplay between temperature, vacancies and quantum effects that determines the behavior of this incommensurate crystal.

We now investigate the permutation effects in the  $^4\text{He}$  crystal with increasing vacancy concentration. Figure 9(a) shows the characteristic peaks and valleys in  $\Delta g_v^{\text{BS}}(r)$  with vacancy number  $n_v = 1, 4$ , and  $8$ . The oscillation amplitude of  $\Delta g_v^{\text{BS}}(r)$  increases with increasing vacancy number, indicating an enhancement of the bosonic character. Figure 9(b) shows  $\delta_x(r)$  defined in Eq. (7) quantifying the permutation effect in the incommensurate solid  $^4\text{He}$  with vacancies. We can see that at low vacancy concentration ( $n_v = 1$ ), the permutation effect is more pronounced at larger interatomic distances ( $\gtrsim 5 \text{ \AA}$ ). Interestingly, as the number of vacancies increases from 1 to 4, the peaks at larger distances (around  $9 \text{ \AA}$ ) are suppressed. However, the permutation effect persists and manifests itself in smaller peaks that are more evenly distributed over the entire range of interatomic distances. This suggests that the bosonic character is more evenly distributed in the crystal when there are more vacancies, even if the specific peak at  $9 \text{ \AA}$  is lowered. What is crucial is that the behavior changes

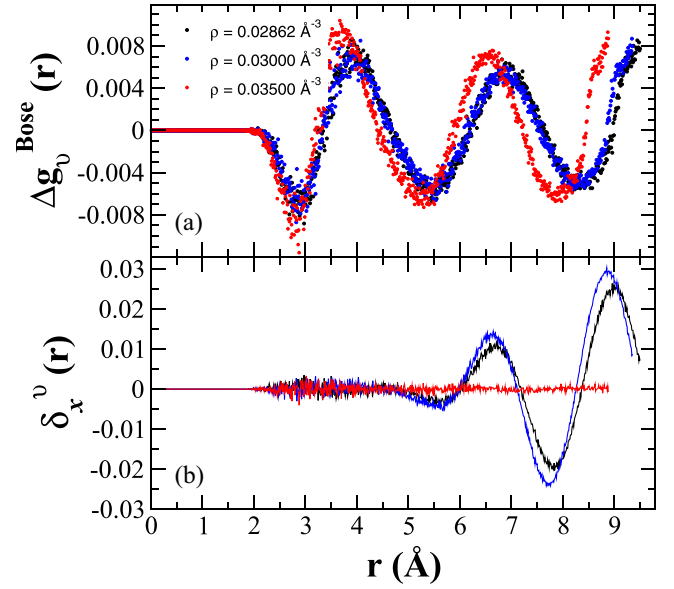


FIG. 10. Pair-correlation function difference for a system with single-vacancy at three different crystal densities (b) the permutation effect on  $g(r)$ . The calculations are carried out at  $T = 0.5 \text{ K}$ .

with vacancy number from 4 to 8. The  $\delta_x^v(r)$  peaks gradually become larger, indicating a stronger and more consistent permutation effect over the entire range of interatomic distances. These peaks also show a size gradient increasing from short distances ( $\approx 3 \text{ \AA}$ ) to larger interatomic distances ( $\approx 9 \text{ \AA}$ ). This suggests that the permutation effect not only becomes stronger as the number of vacancies increases from 4 to 8, but also begins to affect the system more uniformly across all interatomic distances.

However, an additional factor that should be considered is the possible influence of the interaction between vacancies. Previous studies [22,23] suggest that attractive interaction between vacancies in solid  $^4\text{He}$  can lead to the formation of vacancy clusters at higher concentrations. This clustering could significantly influence the observed trends in  $g(r)$ . For instance, if vacancy clusters tend to have a compact structure, they could cause an initial decrease in peak heights at larger distances compared to isolated vacancies, as the interatomic distances within the cluster are reduced. On the other hand, clusters with a more open structure could allow exchange paths on different length scales, leading to unexpected changes in peak heights and valley depths compared to the trends observed at lower vacancy concentrations. Further investigation of the specific nature of vacancy interaction and clustering in our system is necessary to fully understand their influence on the bosonic effect. Overall, Fig. 9(b) provides insights into the complex interplay of vacancy concentration, interatomic distance, and bosonic effect. The initial dominance of the bosonic effect at lower concentrations emphasizes its sensitivity to spatial arrangement.

Finally, we investigate the influence of crystal density on vacancy behavior and permutation effects with a single vacancy at  $T = 0.5 \text{ K}$ . Figure 10(a) shows  $\Delta g_v^{\text{BS}}(r)$  with  $n_v = 1$  for the crystals of different densities. The vacancy signature is present in the crystal; distinct peaks and valleys characterize it

and persist with increasing crystal density. The peaks, mainly the second and third ones, exhibit a leftward shift as the atoms move closer together due to the denser packing, effectively “squeezing” them together around the vacancy. This contraction effect leads to a decrease in peak position by 0.5 Å between the lowest and highest densities. Furthermore, the observed valleys indicate a localized decrease in density compared to a perfect crystal, suggesting a complex interplay of attractive and repulsive forces near the vacancy. Figure 10(b) shows the permutation effect computed by  $\delta_x^v(r)$  using Eq. (7) with  $n_v = 1$ , at different crystal densities. As expected, the permutation effect generally weakens with increasing crystal density and practically disappears at a density of  $0.03500 \text{ \AA}^{-3}$ . Interestingly, when the density changes from  $0.02862 \text{ \AA}^{-3}$  to  $0.03000 \text{ \AA}^{-3}$ , the permutation effect causes a slight increase in both peak and valley heights, accompanied by a shift to the left. This unexpected behavior at intermediate densities (between  $0.02862 \text{ \AA}^{-3}$  and  $0.03000 \text{ \AA}^{-3}$ ) suggests a possible interplay between density-dependent interatomic interactions and quantum statistics. This means that the influence of indistinguishability on the vacancy feature decreases as the crystal becomes denser. In simpler terms, denser packing restricts the “delocalization” characteristic of Bose statistics, where identical atoms tend to blur the influence of vacancy. Consequently, the  $g(r)$  difference shrinks, indicating a weaker influence of quantum statistical effects on vacancy behavior in denser crystals.

#### IV. CONCLUSIONS

Using path-integral Monte Carlo (PIMC) simulations, we have studied the effects of permutations in incommensurate solid  $^4\text{He}$  by comparing the results with both Boltzmann and Bose statistics. This approach allowed us to isolate the unique contributions of the Bose statistics, including permutation effects and implicit statistical treatment differences. We studied the solid  $^4\text{He}$  with densities from  $0.028$  to  $0.035 \text{ \AA}^{-3}$  at temperatures from  $0.2$  to  $2.0$  K and with vacancy concentrations from  $0.55$  to  $5.55\%$  (corresponding to 1 to 10 vacancies in 180 lattice sites).

We find that permutation effects significantly reduce the vacancy formation energy, especially at low densities (e.g.,

$19\%$  reduction at  $0.02862 \text{ \AA}^{-3}$ ). This effect weakens with increasing vacancy concentrations. The permutation effects on the vacancy formation energy show a “steplike behavior” with respect to temperature and density being much less pronounced at higher temperatures (i.e., for  $T \gtrsim 1.0$  K) and higher density. For each additional vacancy, the permutation effect on the vacancy formation energy contributes, on average, a reduction of  $0.82$  K to the vacancy formation energy.

Vacancies induce lattice distortions leading to a local density reduction and a compensatory increase in the neighboring regions, which varies from 1 to 5%. The Bose statistics influence the pair-correlation function at larger distances and leads to peaks and valleys that are about 2% higher or lower than that from the Boltzmann simulations. The influence of Bose statistics and permutation effects on the crystal structure initially increase with increasing the vacancy concentration, but become weak at higher concentration due to high disorder.

These obtained results highlight the crucial role of quantum effects on the properties of solid  $^4\text{He}$  containing vacancies, especially at lower temperatures and lower vacancy concentrations. Moreover, they underscore the need for further investigation to fully understand the underlying mechanisms and to quantify the precise influence of these factors over a wider range of temperatures and vacancy concentrations, especially where the “steplike behavior” becomes more apparent.

#### ACKNOWLEDGMENTS

This research was supported by Brazilian agencies Conselho Nacional de Desenvolvimento Científico e Tecnológico (CNPq), Fundação de Amparo à Pesquisa do Estado de Minas Gerais (FAPEMIG), and Fundação de Amparo à Pesquisa do Estado de São Paulo (FAPESP). R.A. acknowledges Coordenação de Aperfeiçoamento de Pessoal de Nível Superior (CAPES) for the fellowship. The authors thank Prof. David Ceperley for allowing the use of his UPI code and for the fruitful discussions. Additionally, we extend our thanks to the LaMCAD/UFG, and the National Laboratory for Scientific Computing (LNCC/MCTI, Brazil) for providing computational resources of the SDumont supercomputer.

- 
- [1] C. Cazorla and J. Boronat, *Rev. Mod. Phys.* **89**, 035003 (2017).
  - [2] M. H.-W. Chan, R. Hallock, and L. Reatto, *J. Low Temp. Phys.* **172**, 317 (2013).
  - [3] J. Beamish, *J. Low Temp. Phys.* **197**, 187 (2019).
  - [4] R. Hallock, *J. Low Temp. Phys.* **197**, 167 (2019).
  - [5] F. Souris, A. Qu, J. Dupont-Roc, J. Grucker, and P. Jacquier, *J. Low Temp. Phys.* **179**, 390 (2015).
  - [6] F. Souris, J. Grucker, J. Dupont-Roc, and P. Jacquier, *Europhys. Lett.* **95**, 66001 (2011).
  - [7] J. Grucker, *J. Low Temp. Phys.* **197**, 149 (2019).
  - [8] H. J. Maris, *J. Low Temp. Phys.* **155**, 290 (2009).
  - [9] C. Cazorla and J. Boronat, *Phys. Rev. B* **92**, 224113 (2015).
  - [10] L. Pollet, M. Boninsegni, A. B. Kuklov, N. V. Prokof'ev, B. V. Svistunov, and M. Troyer, *Phys. Rev. Lett.* **101**, 097202 (2008).
  - [11] E. L. Pollock and D. M. Ceperley, *Phys. Rev. B* **30**, 2555 (1984).
  - [12] D. M. Ceperley, *Rev. Mod. Phys.* **67**, 279 (1995).
  - [13] R. Storer, *J. Math. Phys.* **9**, 964 (1968).
  - [14] A. D. Klemm and R. Storer, *Aust. J. Phys.* **26**, 43 (1973).
  - [15] D. M. Ceperley and E. L. Pollock, *Phys. Rev. Lett.* **56**, 351 (1986).
  - [16] R. A. Aziz, A. R. Janzen, and M. R. Moldover, *Phys. Rev. Lett.* **74**, 1586 (1995).
  - [17] M. Boninsegni, N. Prokof'ev, and B. Svistunov, *Phys. Rev. Lett.* **96**, 070601 (2006).
  - [18] G. Jacucci and M. Ronchetti, *Solid State Commun.* **33**, 35 (1980).
  - [19] B. Chaudhuri, F. Pederiva, and G. V. Chester, *Phys. Rev. B* **60**, 3271 (1999).
  - [20] F. Pederiva, G. V. Chester, S. Fantoni, and L. Reatto, *Phys. Rev. B* **56**, 5909 (1997).



- [21] V. Z. Pedroso, V. Zampronio, and S. Vitiello, *J. Phys.: Condens. Matter* **33**, 075901 (2021).
- [22] B. K. Clark and D. M. Ceperley, *Comput. Phys. Commun.* **179**, 82 (2008).
- [23] M. Boninsegni, A. B. Kuklov, L. Pollet, N. V. Prokof'ev, B. V. Svistunov, and M. Troyer, *Phys. Rev. Lett.* **97**, 080401 (2006).
- [24] B. A. Fraass, P. R. Granfors, and R. O. Simmons, *Phys. Rev. B* **39**, 124 (1989).
- [25] R. Rota and J. Boronat, *Crystals* **8**, 344 (2018).
- [26] R. Rota and J. Boronat, *Phys. Rev. Lett.* **108**, 045308 (2012).
- [27] G. J. Hyland, G. Rowlands, and F. W. Cummings, *Phys. Lett. A* **31**, 465 (1970).